Polariton-polariton scattering in organic microcavities at high excitation densities

Paolo Michetti*
Institute of Theoretical Physics and Astrophysics, University of Würzburg, D-97074 Würzburg, Germany

G. C. La Rocca†
Scuola Normale Superiore and CNISM, Piazza dei Cavalieri 7, 56126 Pisa, Italy

(Received 7 September 2009; revised manuscript received 5 August 2010; published 27 September 2010)

Polariton-polariton scattering phenomena in organic strongly coupled microcavities have been theoretically assessed on the basis of the kinematic interaction of Frenkel excitons. Experiments have been focused on resonant pumping at magic angle, as well established in inorganic quantum-well microcavities, but insofar no experimental evidence of parametric amplification has been found. Here, we show that in J-aggregate-based microcavities a peculiar polariton-polariton scattering process applies, i.e., the scattering of two resonantly pumped polaritons toward a polariton of lower energy and a localized excitation of the exciton reservoir. This process, because of the localized nature of the final state, is not limited by momentum conservation, and we show that in a high-quality factor microcavity it could be exploited to setup resonant pumping experiments not requiring a magic angle configuration.

DOI: 10.1103/PhysRevB.82.115327 PACS number(s): 78.66.Qn, 71.36.+c, 78.20.Bh, 71.35.Aa

I. INTRODUCTION

Strong coupling in solid-state microcavities (MCs), based on inorganic quantum wells, has been extensively studied.[1,2] In such structures Wannier excitons and photon cavity modes are mixed in coherent light-matter excitations, called polaritons. The strong-coupling regime is signaled by the appearance of two anticrossing dispersion branches, i.e., the lower polariton (LP) branch and the upper polariton branch, whose minimal energy separation is called the Rabi splitting. Early stage experiments were characterized by the presence of a bottleneck effect in polariton thermalization.[3,4] More recently, the success in turning on polariton-polariton scattering (PPS) opened up the way to a number of interesting phenomena, such as parametric processes[5] and polariton condensation.[6,7]

On the other hand organic strongly coupled MCs have been developed since 1998,[8] employing different kinds of optically active organic layers, among which the cyanine dye J-aggregate films are probably the most typical. Organic materials possess Frenkel excitons, instead of Wannier ones, with large binding energy and oscillator strength. Because of this, organic MCs allow obtaining values of the Rabi splitting up to 300 meV (Ref. 9) and offer the possibility of easily observing polaritons at room temperature.[10] Electroluminescence was demonstrated in a J-aggregate strongly coupled microcavity light-emitting diode[11] at room temperature. Peculiar molecular phenomena, like the observation of strongly coupled vibronic replicas has also been also demonstrated.[12] A more detailed review about organic MCs can be found in Refs. 13 and 14.

The nature of polariton in disordered organic MCs has been addressed from the theoretical point of view,[15–18] underlying the coexistence of delocalized and partially localized polaritons, together with a large number of uncoupled excitons, acting as an excitonic reservoir (ER). The mechanism of polariton relaxation due to the interaction with molecular vibrations was discussed in Refs. 19 and 20, and simulation of the radiative decay time of J-aggregate MCs photoluminescence was presented in Ref. 21. The effect of anisotropy in organic crystal was theoretically analyzed,[22] as well as the possible occurrence of nonlinear phenomena,[23] as observed in inorganic MCs, associated to regimes of high polariton density.

The present experimental photoluminescence data of J-aggregate MCs under nonresonant pumping[24] have been explained in terms of a relaxation bottleneck. An initial relaxation step leads to the accumulation of particles in the ER, from which the relaxation is then induced by the emission/absorption of quanta of localized vibrations.[20,25] A different model, but leading to similar conclusions, was developed in Ref. 26 through the application of a quantum kinetic theory, which describes the organic MC dynamics in a regime of nonperturbative coupling of polaritons with resonant optical vibrations.

Given the present stage of experimental evidences, a semiclassical approach can be useful to understand the relevance of phenomena like PPS and the chance in observing parametric processes or even polariton condensation. In this work we setup a minimal model in order to analyze the relevance of exciton-exciton interactions in polariton relaxation at high excitation densities. In particular, we focus on a configuration, in which two resonantly pumped polaritons scatter into a LP bottom (LPB) state and a higher energy ER state, and estimate its efficiency via the Fermi's golden rule.

II. MICROSCOPIC MECHANISM OF POLARITON-POLARITON SCATTERING

In an organic strongly coupled microcavity the photon cavity modes polarize the optically active molecules, giving rise, also in presence of disorder, to almost delocalized ideal exciton polaritons. We assume for simplicity two-level molecules, with resonance energy E_0^{ex}, interacting with the first MC photon mode, with energy dispersion

$$E_k^{ph} = \hbar c_0 \sqrt{k_\perp^2 + k^2}, \tag{1}$$

where c_0 is the light velocity in the medium, $k_\perp$ the confined wave vector, $k = |\vec{k}|$ the modulus of the wave vector in the

MC plane. In the strong-coupling regime light-matter interaction leads to the formation of the polariton dispersion curves

$$E_k = \frac{E_k^{ph} + E_0^{ex}}{2} \pm \sqrt{\Delta^2 + (E_k^{ph} - E_0^{ex})^2} \tag{2}$$

with Δ the Rabi splitting, which is a measure of the coupling strength. A delocalized polariton wave function of wave vector $\vec{k}$ can be described approximatively by the following operator:

$$\Psi_{\vec{k}}^{\dagger} = C_k^{ph} c_{\vec{k}}^{\dagger} + C_k^{ex} \sum_i^N \frac{e^{\imath \vec{k} \vec{r}_i}}{\sqrt{N}} b_i^{\dagger} \tag{3}$$

with $c_{\vec{k}}^{\dagger}$ and $b_i^{\dagger}$, respectively, the photon and molecular exciton operators, C_k^{ex} and C_k^{ph} given by the usual Hopefield coefficients,[1] N the number of molecules. We note that the Hopefield coefficients, like the polariton dispersion curve, depend only on the wave vector modulus k, rather than on the actual wave vector $\vec{k}$. Exciton and photon components satisfy $|C_k^{ex}|^2 + |C_k^{ph}|^2 = 1$ with

$$|C_k^{ex}|^2 = \frac{\Delta^2}{\Delta^2 + (E_k - E_0^{ex})^2}. \tag{4}$$

The exciton-exciton interaction in organic microcavity is due essentially to the Paulion character of molecular excitons, which causes the saturation of their oscillator strength. Al least for the purpose of the present work, the exciton-exciton Hamiltonian can essentially be schematized as the following:[23,27]

$$H_{ex\text{-}ex} = \varepsilon \sum_i^N b_i^{+} b_i^{+} b_i b_i. \tag{5}$$

In organic microcavities ideal-like delocalized polaritons, described by their usual upper and lower dispersion curves, coexist together with localized excitations. These localized excitations $|I\rangle$ have a finite extent, which guarantees their orthogonality to the delocalized polaritons. We describe them as

$$|I\rangle = \sum_i \phi_i^{(I)} |i\rangle \tag{6}$$

with $\phi_i^{(I)}$ giving the exciton component on the ith molecular site and $|i\rangle = b_i^{\dagger}|0\rangle$. Only a fraction on the order of 10^{-4} of the excited states are delocalized polaritons while the remaining part form a huge ER, quite similar to the bare film exciton density of states (DOS).[15,20] The presence of the ER allows a channel of polariton-polariton scattering, leading from two initial lower branch ideal-like delocalized polaritons to a polariton final state of lower energy and a final state in the exciton reservoir, as shown in Fig. 1. The exploitation of this process in resonant pumping experiments has no need of a magic angle configuration, due to the localized nature of the ER final state, which relaxes momentum-conservation rule.

We apply Fermi's golden rule (see, however, the discussion below) to compute the polariton-polariton scattering rates and distinguish the processes where initial and final

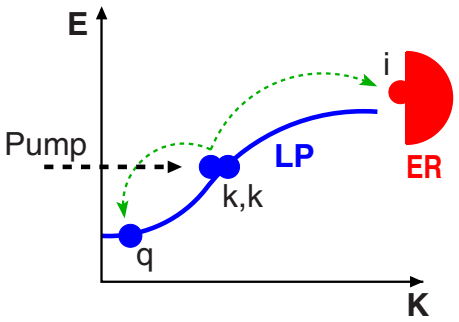

FIG. 1. (Color online) Sketch of a resonant pumping situation which activates the polariton-polariton scattering process leading to the population of final states on the LP bottom and on the ER.

states are delocalized polaritons $(\vec{k}, \vec{k}' \to \vec{q}, \vec{q}')$ or where the final states are instead a polariton and an ER localized state $(\vec{k}, \vec{k}' \to q, I)$. We will use the notation $|\vec{k}\rangle = \Psi_{\vec{k}}^{\dagger}|0\rangle$. The core of the calculation of the polariton-polariton scattering rates via Fermi's golden rule is, for the first process, the element of the interaction Hamiltonian [Eq. (5)] between initial states $|\vec{k}\vec{k}'\rangle$ and final two polariton states $|\vec{q}\vec{q}'\rangle$

$$\langle \vec{q}\vec{q}' | H_{ex\text{-}ex} | \vec{k}\vec{k}' \rangle = \varepsilon \frac{C_k^{ex} C_{k'}^{ex} C_q^{ex} C_{q'}^{ex}}{N^2} \sum_i^N e^{\imath(\vec{q}+\vec{q}'-\vec{k}-\vec{k}')\vec{r}_i} \tag{7}$$

with $|\vec{k}\rangle$ given by the polariton creation operator in Eq. (3). If we instead consider the second process with a final state composed by a polariton and a reservoir exciton $|\vec{q}I\rangle$, we obtain

$$\langle \vec{q}I | H_{ex\text{-}ex} | \vec{k}\vec{k}' \rangle = \varepsilon \frac{C_k^{ex} C_{k'}^{ex} C_q^{ex}}{N^{3/2}} \eta_I \tag{8}$$

with

$$\eta_I = \sum_i e^{\imath(\vec{q}-\vec{k}-\vec{k}')\vec{r}_i} \phi_i^{(I)}. \tag{9}$$

This factor represents the overlap of three quasi-ideal polaritons and one localized exciton. For fully localized excitations, which are described by $\phi_i^{(I)} = \delta_{i,I}$ (i.e., $|I\rangle = |i\rangle$), $|\eta_I|$ would be unitary. However, even if small, the states of the exciton reservoir possess a finite extent. Then, it is convenient to introduce the parameter $\eta = \sqrt{\langle |\eta_I|^2 \rangle}$ obtained by averaging over the states of the ER. We numerically estimate η for the case of a one-dimensional MC with the model described in Ref. 16. All eigenstates of a strongly coupled microcavity are calculated in the presence of diagonal energetic disorder on the exciton resonance with a standard deviation of 30 meV. We then compute η, averaging over all the ER states, obtaining the estimate $\eta \approx 10^{-1}$. It would be numerically much more demanding to estimate η for a two-dimensional (2D) MC and, considering also the uncertainty in the disorder characterization, in the following we will adopt η as a free parameter of the model.

Now the scattering rates for the two processes, respectively, read

$$W_{\vec{k}\vec{k}'\to\vec{q}\vec{q}'} = \mathcal{W}\frac{|C^{ex}_{q'}|^2}{N}\left|\sum_i^N e^{\imath(\vec{q}+\vec{q}'-\vec{k}-\vec{k}')\vec{r}_i}\right|^2 \delta_{(E_{k'}+E_k-E_q-E_{q'})},$$

$$= \mathcal{W}N|C^{ex}_{q'}|^2\delta_{(\vec{q}+\vec{q}'-\vec{k}-\vec{k}')}\delta_{(E_{k'}+E_k-E_q-E_{q'})}, \quad (10)$$

and

$$W_{\vec{k}\vec{k}'\to\vec{q}I} = \mathcal{W}|\eta_I|^2\delta_{(E_{k'}+E_k-E_q-E_I)}, \quad (11)$$

where $\mathcal{W}=\frac{2\pi\varepsilon^2}{\hbar}\frac{|C^{ex}_k C^{ex}_{k'} C^{ex}_q|^2}{N^3}$ and $\delta_{(E)}$ is the Dirac delta ensuring energy conservation. The two processes mainly differ for the fact that, while the former have to fulfill both momentum and energy conservation, the latter only requires energy conservation. This fact is qualitatively different with respect to the polariton-polariton scattering processes typical of inorganic microcavities. In particular, in Eq. (11) the vectorial nature of $\vec{k}$, $\vec{k}'$, and $\vec{q}$ is immaterial, but only energy matters. Therefore, a chosen $\vec{k}$ can scatter with every polariton of wave-vector modulus k', ending up in every polariton of wave-vector modulus q with the same probability.

Within first-order perturbation theory, if all conservation laws are satisfied and taking into account that the number of final states I in the ER is huge ($\approx N$) with respect to the number of polariton states, the ratio of the two relaxation channel rates would be given by η^2. For the process involving localized states, perturbation theory is applicable, and we have checked up to third order that the rate given by Eq. (11) remains adequate. For the process involving delocalized state, however, the Fermi's golden rule is generally not sufficient to calculate the scattering rate and, at least for processes involving polaritons having small wave vectors, it can be shown that the estimate given by Eq. (10) should also be suppressed by a factor which numerically is typically of the same order of η^2.[23,28]

Depending on the pumping energy we can expect one or the other of the two PPS processes to prevail. Magic angle experiments, exploiting the first PPS process, have not been successful till now in organic MCs. The main difficulty seems related to the Rayleigh scattering of pumping light entering the MC mirrors, which leads to a randomization of the population inside the whole annular region k, resonant with the pumping laser. In other terms, in amorphous organic MCs, disorder easily induces a mixing between the degenerate states inside an annular region of the same k. On the other hand, the second PPS process, not requiring momentum conservation, is totally unaffected by this issue. In particular, the second process is active, only for energies on the upper half of the LP branch spectral span, and, when we are not fulfilling the magic angle configuration, it is expected to be predominant. For lower energies only the first PPS process remains active. In the following, we will focus on the region where the second PPS is active and, for simplicity, we will ignore the first PPS. We cannot exclude a quantitative contribution of the first PPS, but we are more interested in describing the qualitatively different features of the second PPS relaxation channel.

III. RESONANT PUMPING

Let us imagine now a resonant pumping situation in which the PPS in Eq. (11) could be exploited in order to drive population at the bottom of the lower polariton branch. The ER DOS for two-level molecules can be approximately described by a Gaussian distribution: $D_{\mathrm{ER}}(E_I) = \frac{N}{\sigma\sqrt{2\pi}}e^{-(E_I-E_0^{ex})^2/2\sigma^2}$, peaked on the naked exciton energy E_0^{ex}, with a standard deviation σ, which describes the inhomogeneous broadening of the resonance. To satisfy energy conservation we can pump population at the middle of the energy span of the LP branch: in an annular region corresponding to the wave-vector modulus k (see Fig. 1). The PPS which leads from 2 k polaritons, to a LP state of wave-vector modulus q, near the LPB, and to the Ith exciton in the ER will therefore result close to resonance.

We estimate the rate at which polariton-polariton scattering depopulates the k state by integrating Eq. (11), over all possible polariton q and exciton I final states

$$\int dE_q \int dE_I D(E_q) D_{\mathrm{ER}}(E_I) W_{2k\to q,I}(E_q,E_I). \quad (12)$$

We adopt effective-mass approximation for the LP bottom, for which its DOS becomes

$$D(E) = mR^2N/(\pi\hbar^2) \quad (13)$$

with R the mean molecular distance and $m/(\pi\hbar^2)$ the 2D DOS for the bottom of the polariton branch. Here we disregard the effect of the homogeneous width of polariton states because a smoothening is already accounted by the energetic distribution of the ER states. Performing the integration in Eq. (12), we are led to the following overall scattering rate for the polariton-polariton process:

$$\frac{1}{\tau_{p\text{-}p}} = \frac{\mathcal{W}\eta^2}{N}\left[\frac{1}{2}+\frac{1}{2}\mathrm{erf}\left(\frac{2E_k - E_0^{ex} - E_{\mathrm{LP}}^{bot}}{\sigma\sqrt{2}}\right)\right] \quad (14)$$

with $\mathcal{W}\approx 1.6\times 10^{16}$ s^{-1}, estimated with the typical values of $m=10^{-5}m_e$, $\varepsilon=2$ eV, $R=20$ nm, $|C^{ex}_{\mathrm{LPB}}|^2=0.1$, and $|C^{ex}_k|^2=0.5$.

Now we introduce some notations that will be useful to develop a numerical model for the resonant pumping simulation. Let us call $f_{(E)}$ the population distribution function over the LP branch while $D_{(E)}$ the full polariton DOS, therefore $N_{(E)}=D_{(E)}f_{(E)}$ corresponds to the polariton population density over the LP branch. In the annular region k we will find a population density $N_{(E_k)}$, which could scatters with the population density in k' (i.e., $N_{(E_{k'})}$). The scattering events taking places in a time unit are

$$N_{(E_k)}N_{(E_{k'})}W_{kk'\to qI}D_{(E_q)}[1+f_{(E_q)}]D_{\mathrm{ER}}(E_I)dE^4_{k,k',q,I}$$

with $dE^4_{k,k',q,i}=dE_k dE_{k'} dE_q dE_I$. Note that we added the Bosonic final-state stimulation for the polariton state q. To satisfy particle conservation, the rate of this process should correspond to the population derivatives

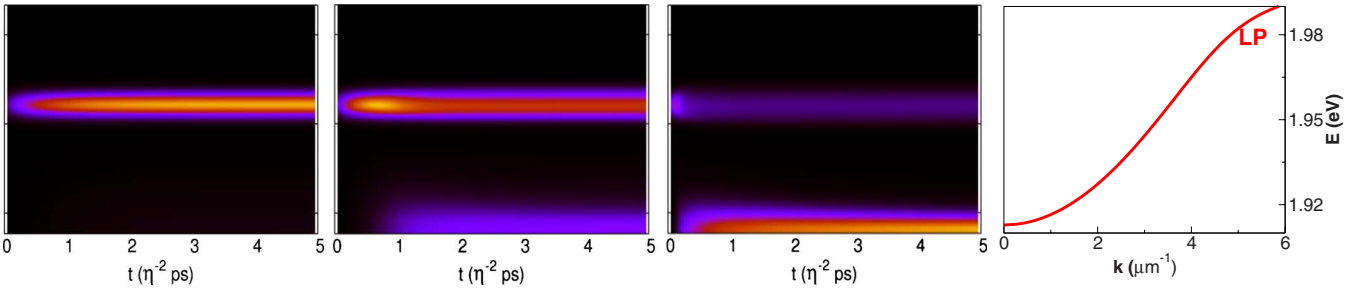

FIG. 2. (Color online) Time-dependent population for a continuous pumping with rates of $\eta^2 10^{10}$, $\eta^2 10^{11}$, and $\eta^2 10^{12}$ particle for second for site (respectively, from left to right). The population on the spectral range of the LP is represented in a color plot, for time up to $5\eta^{-2}$ ps. The picture on the right side represents the LP dispersion curve.

$$\frac{dN_{(E_q)}}{dt} = \frac{dN_{(E_I^{ex})}}{dt} = -\frac{dN_{(E_k)}}{dt} = -\frac{dN_{(E_{k'})}}{dt}.$$

We can now formulate a rate equation for the distribution function as

$$\frac{d}{dt} f_{(E)} = -\gamma_E f_{(E)} + p_E + \int dE_{k'} dE_I dE_k \times [\mathcal{P}_{in}^{(E,E_I,E_k,E_{k'})} - \mathcal{P}_{out}^{(E_{k'},E_I,E_k,E)}] \quad (15)$$

with

$$\mathcal{P}_{in}^{(E,E_I,E_k,E_{k'})} = [1 + f_{(E)}] D_{\mathrm{ER}}(E_I) N_{(E_k)} N_{(E')} W_{k,k' \to q,I}, \quad (16)$$

$$\mathcal{P}_{out}^{(E_{k'},E_I,E_k,E)} = D_{(E')}[1 + f_{(E')}] D_{\mathrm{ER}}(E_I) N_{(E_k)} f_{(E)} W_{k,q \to k',I}, \quad (17)$$

where $\gamma_E = \frac{|C_E^{ph}|^2}{\tau}$ is the polariton radiative decay rate and τ the photon confinement time of the MC. The system is driven by the resonant pumping p_E, from which follows that the overall number of particle injected in the MC in the time unit is $P = \int p_E D_{(E)} dE$. We note that being the vectorial nature of polaritons not important in the present process, there exists a biunique relationship between the wave-vector modulus q and energy $E = E_q$ given by the LP dispersion curve [Eq. (2)], which has cylindrical symmetry. Therefore a LP polariton can either be identified by its energy E or by its wave vector q. Other scattering processes such as scattering with emission and absorption of phonon are here neglected for simplicity, assuming a regime in which PPS and radiative decay are the only leading phenomena. This is consistent with a resonant pumping situation in which a high polariton density is driven on the PB branch, turning on PPS phenomena.

We numerically implemented the rate equations Eq. (16) for the full LP branch with a time-dependent calculation of $f_{(E;t)}$. The time-dependent population density $N_{(E)}$, for a microcavity with detuning of 80 meV and Rabi splitting of 100 meV, with $\tau = 300\eta^{-2}$ fs, is shown in Fig. 2 for a continuous resonant pump $p = P/N$ of $\eta^2 10^{10}$, $\eta^2 10^{11}$, and $\eta^2 10^{12}$, expressed as the total particle number injected in the MC for second for molecular site. The three pictures well show the transition from an "empty" regime, where the scattering toward the bottom of the LP branch is negligible, to an "accumulation" regime, where PPS is predominant over radiative decay and the injected population is accumulated at the LP bottom.

We simulated also the effect of a resonant pulsed pump of Gaussian shapelike in Fig. 3, centered on $t = 1\eta^{-2}$ ps with standard deviation of $300\eta^{-2}$ fs, corresponding to the photon confinement time of the MC. Initially the k state of energy about 1.96 eV is populated by the pulse, but when the polariton density becomes sufficiently high PPS is activated and a sudden population transfer takes place from the state k to the LPB state q, corresponding to about 1.91 eV. From now on the photon injected in the MC is directly led by PPS toward the LP bottom where it accumulates while only a small part of the population remains on the pumped states. Finally, after the pumping pulse, the polariton population decays due to photoluminescence emission.

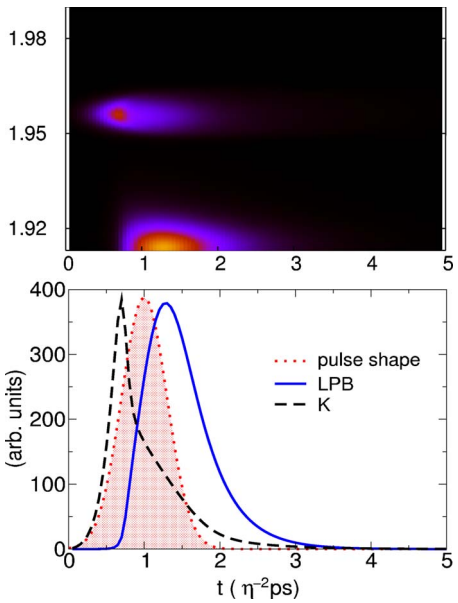

FIG. 3. (Color online) Polariton population following a pulsed resonant pumping described by the filled Gaussian shape in the lower picture. In the upper figure we show a color plot of the population density on the LP branch as a function of time. In the lower picture we show the time profile of the population corresponding to the resonantly pumped state (k) and to the bottom state of the LPB.

IV. THREE STATES MODEL

In this section we derive an analytical model for the PPS in resonant pumping conditions. As before, we will assume a resonant pumping on the spectral region of the LP branch intermediate at halfway point between the LPB and the ER, generating polaritons k (Fig. 1). With this choice of the resonant pumping, due to energy conservation, the PPS final states are one at the LPB and one in the ER. With the assumption for the PPS to be the dominant process, the only parts of the system effectively populated will be the resonantly pumped region (k states) and the final states in the exciton reservoir (r states) and the lower polariton bottom (b states). We model therefore the resonant pumping experiment with a system of scattering rate equations for three spectral regions represented by three states: b, k, and r. The system of rate equations is the following:

$$\frac{d}{dt}N_k = -\gamma_k N_k - 2\left(1+\frac{N_b}{a}\right)\mathcal{W}\eta^2\frac{N_k^2}{N} + P,$$

$$\frac{d}{dt}N_b = -\gamma_b N_b + \left(1+\frac{N_b}{a}\right)\mathcal{W}\eta^2\frac{N_k^2}{N},$$

$$\frac{d}{dt}N_r = -\gamma_r N_r + \left(1+\frac{N_b}{a}\right)\mathcal{W}\eta^2\frac{N_k^2}{N} \tag{18}$$

with γ the radiative (or nonradiative) decay rate for polariton and ER, respectively, P the total number of particle injected in the system in the time unit by resonant pumping, a an effective number of different states populated at the LPB spectral region. The rate of the PPS process ($\frac{1}{\tau_{p\text{-}p}} \approx \frac{\mathcal{W}\eta^2}{N}$) is calculated by Eq. (12), obtaining Eq. (14). a can be estimated integrating the polariton DOS in the phase space (in energy) near the LPB accessible to the PPS process $(k,k \to q,I)$

$$a = \int dE_q \int dE_I D_{(E_q)} \frac{1}{\sigma\sqrt{2\pi}} e^{-(E_I - E_0^{ex})^2/2\sigma^2} \delta_{(2E_k - E_q - E_I)}$$
$$= \frac{mR^2}{N\hbar^2}\left[\frac{1}{2} + \frac{1}{2}\mathrm{erf}\left(\frac{2E_k - E_0^{ex} - E_{\mathrm{LP}}^{bot}}{\sigma\sqrt{2}}\right)\right] \tag{19}$$

with $E_{\mathrm{LP}}^{bot} = E_{k=0}$ is the bottom of the LP dispersion curve. In the presence of an important population density on the LPB (N_b particle distributed among a states), the polariton-polariton process suffers Bosonic final-state stimulation with an acceleration of a factor $1+\frac{N_b}{a}$. If the population at the bottom is sufficiently high, a number of secondary-relaxation processes may become active and the population of the bottom LP branch can be further concentrated on few lowest laying states. However, here we neglect this possibility, and we make the pejorative assumption, in view of obtaining an accumulation at the LPB, of a populated LPB states. In order to keep the model analytical, we neglect also the return of the ER population on the polariton states, which is also a pejorative assumption. At this point, the last equation is immaterial and only the former two need to be simultaneously solved in order to determines the population in the k and the b regions.

We start from the steady-state condition

$$0 = -\gamma_k n_k - 2\left(1+\frac{n_b}{\alpha}\right)\mathcal{W}\eta^2 n_k^2 + p, \tag{20}$$

$$0 = -\gamma_b n_b + \left(1+\frac{n_b}{\alpha}\right)\mathcal{W}\eta^2 n_k^2, \tag{21}$$

where $n_{k(b)} = N_{k(b)}/N$ is the density of population for site, i.e., density for an area R^2, $\alpha = a/N$ the number of final bottom states for site, and p the pumping rate for site. From the second we obtain

$$\left(1+\frac{n_b}{\alpha}\right)\mathcal{W}\eta^2 n_k^2 = \gamma_b n_b$$

that can be substituted in the first one yielding

$$-\gamma_k n_k - 2\gamma_b n_b + p = 0$$

and therefore

$$n_k = r - t n_b, \tag{22}$$

where we define the ratios

$$r = p/\gamma_k,$$

$$s = \eta^{-2}\gamma_b/\mathcal{W},$$

$$t = 2\gamma_b/\gamma_k,$$

$$\kappa = r/t,$$

$$\omega = s/t^2.$$

Substituting n_k in Eq. (21) we are now reconducted to an equation containing the only variable n_b

$$-s n_b + \left(1+\frac{n_b}{\alpha}\right)(r - t n_b)^2 = 0.$$

After a simple manipulation we obtain the third-order equation

$$n_b^3 + n_b^2(\alpha - 2\kappa) + n_b(\kappa^2 - 2\alpha\kappa - \alpha\omega) + \alpha\kappa^2 = 0. \tag{23}$$

We employ Cardano's formulas to obtain an analytical solution of Eq. (23), and therefore the population at the lower polariton bottom as a function of the pumping intensity. In Fig. 4 we present the fraction of the excited population n_b/n_{tot} in steady-state conditions as a function of the pumping intensity, for a photon confinement time from $50\eta^{-2}$ to $450\eta^{-2}$ fs. We cut from the picture states corresponding to a total density of excitation per site larger than 0.1, which is a generous stability limit for the sample. The picture clearly indicates the transition between a regime of negligible population on the LPB (empty regime) to a regime of accumulation, in which almost the 100% of the excited states are collected at the bottom of the LP branch.

Between the steady-state populations n_b and n_k we find the following relation:

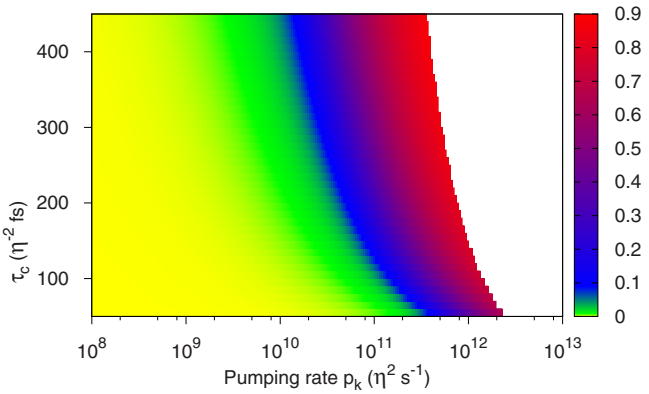

FIG. 4. (Color online) Fraction of the population in the LP bottom in steady-state conditions as a function of the resonant pumping intensity for a microcavity with σ=30 meV for different values of the photon confinement time. As a stability limit, we cut away the region in which the total population of the system exceeds the 10% of the actual number of molecular aggregates.

$$\gamma_k \frac{dn_k}{dp} + 2\gamma_b \frac{dn_b}{dp} - 1 = 0 \tag{24}$$

from which we can clearly identify two limiting conditions of empty and accumulation regimes. In the empty regime the scattering toward the LP branch is negligible and a linear relation links the pumped population n_k with the pump term p, which can be resumed by $\frac{dn_k}{dp} \approx \frac{1}{\gamma_k}$ and $\frac{dn_b}{dp} \approx 0$. In the accumulation regime instead the relaxation processes toward the bottom states are predominant and an increase in the pumping power leads to larger n_b, i.e., the injected population is accumulated at the LP bottom. Such regime is characterized by $\frac{dn_k}{dp} \approx 0$ and $\frac{dn_b}{dp} \approx \frac{1}{2\gamma_b}$. To more clearly mark such transition we identify a threshold pumping value, for which the conditions

$$\frac{dn_k}{dp} \approx \frac{1}{2\gamma_k},$$

$$\frac{dn_b}{dp} \approx \frac{1}{4\gamma_b} \tag{25}$$

are satisfied. In Fig. 5 we show the threshold defined by Eq. (25), as a function of the photon confinement time, for three different values of the disorder parameter σ.

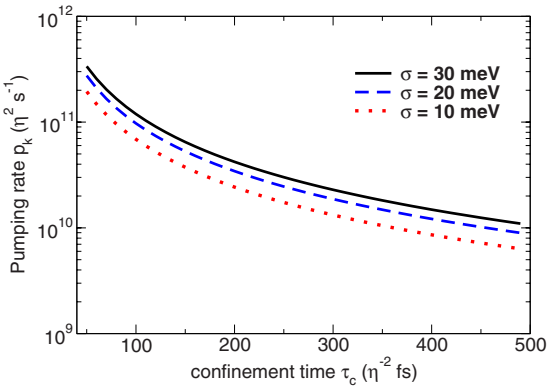

FIG. 5. (Color online) Threshold that marks the transition between the empty and the accumulation regimes, as explained in the text by Eq. (25), for a disorder strength of σ=10, 20, and 30 meV.

V. CONCLUSION

We studied the polariton-polariton scattering in organic microcavities at high excitation densities, emphasizing the presence of a mechanism, originating in the coexistence of delocalized polaritons with a reservoir of quasilocalized molecular excitons. This polariton-polariton scattering process has the peculiarity of not requiring momentum conservation, and thus only energy conservation have to be fulfilled. Therefore, in principle, it can be observed without recurring to the magic angle configuration, employed in inorganic microcavities. We theoretically analyzed, with a semiclassical approach, the possibility of exploiting this scattering process in a resonant pumping experiment, both with continuous and pulsed resonant excitations. We described the transition between an empty pumping regime, where the process is ineffective, to an accumulation regime, where a large population is induced at the lower polariton bottom. The numerical results and, in particular, this transition have also been rationalized in terms of an analytical three states model.

ACKNOWLEDGMENT

We gratefully acknowledge support of the European Commission via Grant No. FP7-PEOPLE-ITN-2008-237900 (ICARUS). P. M. acknowledges financial support from the DFG via the Emmy Noether program.

*michetti@physik.uni-wuerzburg.de
†larocca@sns.it

[1] A. Kavokin and G. Malpuech, *Cavity Polaritons*, Thin Films and Nanostructures Vol. 32 (Elsevier, San Diego, 2003).
[2] *The Physics of Semiconductor Microcavities*, edited by B. Deveaud (Wiley-WCH, Weinheim, 2007).
[3] R. P. Stanley, R. Houdre, C. Weisbuch, U. Oesterle, and M. Ilegems, Phys. Rev. B **53**, 10995 (1996).
[4] F. Tassone, C. Piermarocchi, V. Savona, A. Quattropani, and P. Schwendimann, Phys. Rev. B **56**, 7554 (1997).
[5] P. G. Savvidis, J. J. Baumberg, R. M. Stevenson, M. S. Skolnick, D. M. Whittaker, and J. S. Roberts, Phys. Rev. Lett. **84**, 1547 (2000); M. Saba, C. Ciuti, J. Bloch, V. Thierry-Mieg, R. Andre, L. S. Dang, S. Kundermann, A. Mura, G. Bongiovanni, J. L. Staehli, and B. Deveaud, Nature (London) **414**, 731 (2001).
[6] J. Kasprzak, M. Richard, S. Kundermann, A. Baas, P. Jeambrun, J. M. J. Keeling, F. M. Marchetti, M. H. Szymanska, R. Andre, J. L. Staehli, V. Savona, P. B. Littlewood, B. Deveaud, and L. S.

Dang, Nature (London) **443**, 409 (2006).
[7] J. Kasprzak, D. D. Solnyshkov, R. André, L. S. Dang, and G. Malpuech, Phys. Rev. Lett. **101**, 146404 (2008).
[8] D. G. Lidzey, D. D. C. Bradley, M. S. Skolnick, T. Virgili, S. Walker, and D. M. Whittaker, Nature (London) **395**, 53 (1998).
[9] P. A. Hobson, W. L. Barnes, D. G. Lidzey, G. A. Gehring, D. M. Whittaker, M. S. Skolnick, and S. Walker, Appl. Phys. Lett. **81**, 3519 (2002).
[10] D. G. Lidzey, D. D. C. Bradley, T. Virgili, A. Armitage, M. S. Skolnick, and S. Walker, Phys. Rev. Lett. **82**, 3316 (1999).
[11] J. R. Tischler, M. S. Bradley, V. Bulovic, J. H. Song, and A. Nurmikko, Phys. Rev. Lett. **95**, 036401 (2005).
[12] R. J. Holmes and S. R. Forrest, Phys. Rev. Lett. **93**, 186404 (2004).
[13] R. J. Holmes and S. R. Forrest, Org. Electron. **8**, 77 (2007).
[14] D. G. Lidzey, in *Electronic Excitations in Organic Based Nanostructures*, Thin Films and Nanostructures Vol. 31, edited by V. M. Agranovich and F. Bassani (Elsevier, San Diego, 2003), Chap. 8.
[15] V. M. Agranovich, M. Litinskaia, and D. G. Lidzey, Phys. Rev. B **67**, 085311 (2003).
[16] P. Michetti and G. C. La Rocca, Phys. Rev. B **71**, 115320 (2005).
[17] V. M. Agranovich and Y. N. Gartstein, Phys. Rev. B **75**, 075302 (2007).
[18] P. Michetti and G. C. La Rocca, Physica E (Amsterdam) **40**, 1926 (2008).
[19] M. Litinskaya, P. Reineker, and V. M. Agranovich, J. Lumin. **110**, 364 (2004); **119-120**, 277 (2006).
[20] P. Michetti and G. C. La Rocca, Phys. Rev. B **77**, 195301 (2008).
[21] P. Michetti and G. C. La Rocca, Phys. Status Solidi C **6**, 403 (2009).
[22] H. Zoubi and G. C. La Rocca, Phys. Rev. B **71**, 235316 (2005).
[23] H. Zoubi and G. C. La Rocca, Phys. Rev. B **72**, 125306 (2005); **77**, 159905(E) (2008); H. Zoubi, *ibid.* **74**, 045317 (2006); H. Zoubi and G. C. La Rocca, *ibid.* **76**, 035325 (2007).
[24] S. Ceccarelli, J. Wenus, M. S. Skolnick, and D. G. Lidzey, Superlattices Microstruct. **41**, 289 (2007).
[25] P. Michetti and G. C. La Rocca, Phys. Rev. B **79**, 035325 (2009).
[26] J. Chovan, I. E. Perakis, S. Ceccarelli, and D. G. Lidzey, Phys. Rev. B **78**, 045320 (2008).
[27] V. M. Agranovich and B. S. Toshich, Sov. Phys. JETP **26**, 104 (1968).
[28] M. Litinskaya, Phys. Rev. B **77**, 155325 (2008).